Wall-pressure spectra models for supersonic and hypersonic turbulent boundary layers.

K. Ritos[a,*], D. Drikakis[b,*], I. W. Kokkinakis[a]

[a] *Department of Mechanical and Aerospace Engineering, University of Strathclyde, Glasgow, UK*
[b] *University of Nicosia, Nicosia, Cyprus*

Abstract

This paper presents an investigation of pressure fluctuations spectra beneath supersonic and hypersonic turbulent boundary layers at zero pressure gradient. High-order implicit Large Eddy Simulations have been used to provide numerical data for assessing existing models and further improving their qualitative accuracy in predicting wall-pressure spectra. Several different models have been investigated and it is shown that existing models fail to capture the correct behaviour of pressure fluctuations in supersonic and hypersonic boundary layers across a broad range of frequencies. The models have been modified by introducing compressibility corrections. The modified models are validated against implicit Large Eddy Simulations, Direct Numerical Simulations, and experimental data. The qualitative accuracy of the models is discussed and the most promising model is identified.

Keywords: compressible, supersonic, hypersonic, acoustic loading, spectra models

Nomenclature

α Constant of Chase model

γ Ratio of specific heats

*Corresponding author
Email addresses: konstantinos.ritos@strath.ac.uk (K. Ritos), drikakis.d@unic.ac.cy (D. Drikakis)

γ_M Constant of Chase model

δ (mm) Boundary layer thickness

δ^* (mm) Boundary layer displacement thickness

θ (mm) Boundary layer momentum thickness

μ_M Constant of Chase model

ν_∞ (m^2/s) Free stream kinematic viscosity

ν_w (m^2/s) Kinematic viscosity near the wall

ρ_∞ (kg/m^3) Free stream density

ρ_w (kg/m^3) Near wall density

τ_w Shear stress near the wall

$\Phi(\omega)$ (Pa^2 s/rad) Power spectral density of surface pressure fluctuations

ω (rad/s) Angular frequency

ω_0 (rad/s) Typical angular frequency

$\bar{\omega}$ Dimensionless frequency

α, β Parameters of Efimtsov model

$a, \beta_c, d, e, h^*, d^*, \Delta$ Parameters of Lee model

$a - h$ Parameters of Hu model

a_+ Constant of Chase model

A_{1-4} Constants of Maestrello model

b Constant of Chase model

C_f Coefficient of friction

C_M Constant of Chase model

C_R Scaling factor

C_T Constant of Chase model

C_{1-3} Constant of Goody model

C_{RG} Exponent factor

f (Hz) Frequency

f_0 (Hz) Characteristic frequency

F_C Friction coefficient

H Shape factor

h_w/h_{aw} Ratio of specific enthalpy between normal and adiabatic wall conditions

K_{1-4} Constants of Maestrello model

M Mach number

P'_{rms} (Pa) Pressure fluctuation intensity

q_∞ (Pa) Free stream dynamic pressure

r Adiabatic recovery factor

R_T Ratio of the outer to inner boundary layer time scale

Re_τ Friction Reynolds number

Re_θ Reynolds number based on θ

Re_x Reynolds number based on distance x

Sh Strouhal number

T_∞ (K) Free stream temperature

T_w (K) Near wall temperature

U_∞ (m/s) Free stream velocity

u_τ (m/s) Friction velocity

U_c Velocity used in Chase model

x (mm) Distance from the leading edge of the plate to the point of spectra calculations

1. Introduction

Wall pressure fluctuations beneath hypersonic turbulent boundary layers (TBL) are major sources of vibration and acoustic fatigue on aerospace structures. Hypersonic aircraft design requires accurate estimation of the acoustic loading on various surfaces of the aircraft. Semi-empirical wall-pressure spectra models (WPSM) can provide an estimate of the pressure fluctuations at a reduced cost compared to wind tunnel experiments and high fidelity simulations.

Various WPSM have been developed based on experimental measurements, theoretical analysis and numerical simulations. Past studies have focused on low speed flows with the compressibility effects neglected [1, 2, 3], or weak compressibility effects were taken into account [4, 5, 6, 7]. More recent papers have introduced the effects of favourable and adverse pressure gradient [8, 9] without considering high-speed compressible flows. Existing models may provide an accurate description of the pressure fluctuations for incompressible flows, however, fail to predict the spectra in supersonic and hypersonic TBL, as the results of this study also show. Although there is a need for a rigorous modelling development for both low and high speed flows, the existing modelling framework can still be improved by taking into account compressibility effects associated with supersonic and hypersonic TBL.

In this paper, the qualitative accuracy of several WPSM is assessed for supersonic and hypersonic TBL. WPSM are compared with data that has been obtained from implicit Large Eddy Simulations (iLES)[10, 11], which can be considered as an under-resolved Direct Numerical Simulation (DNS). Furthermore, compressibility corrections are proposed that significantly improve the accuracy of spectra models.

2. iLES data

The iLES data has been calculated in the framework of the high-order code CNS3D, which has been validated in several iLES studies of transitional and turbulent flows [12, 13, 14, 10, 11, 15]. CNS3D is based on the HLLC

Riemann solver [16] and a ninth-order WENO scheme [17] for the advective terms, second-order discretisation for the viscous terms and the third-order accurate Runge-Kutta method for the time integration [18].

It has been shown that shock-capturing, finite volume, Godunon-type methods are suited for the simulation of compressible turbulent flows in the numerical framework of iLES [18, 19]. Furthermore, the order of spatial discretization in iLES significantly influences the turbulence scales captured [20, 11]. A detailed account of the accuracy of iLES results beneath supersonic TBL has been published in [21, 10].

In this paper, we have investigated supersonic and hypersonic flows at Mach numbers $M = 2.25$, $M = 4$, and $M = 8$. The configuration comprises a zero-pressure gradient flow over a flat plate with no shock-boundary-layer interactions. The flow parameters are given in Table 1, as well as in [10, 11]. The power spectral density of the pressure fluctuations has been calculated using Welch's method [22]. The sampling frequency is approximately 15.5, 420 and 550 MHz for each Mach number (in increasing order), respectively, based on the time-step of each simulation: 65, 2.4 and 1.8 ns. The effective resolution due to mesh restrictions being approximately 3.5 MHz (2.7×10^7 rad/s). This frequency is high enough to resolve all the spectrum regions that contain the most energetic pressure fluctuations. In all cases the $\Delta y_w^+ \sim 0.5$, or less, ensuring all viscous effects are captured. Additional details regarding the mesh resolution, mesh spacing in wall units and mesh convergence are given in [10, 11].

M	x (mm)	U_∞ (m/s)	ρ_∞ (kg/m^3)	T_∞ (K)	ν_∞ (m^2/s)	δ (mm)	δ^* (mm)	θ (mm)	u_τ (m/s)
2.25	61	588	0.49	170	2.39×10^{-5}	1.08	0.3	0.09	29.5
4.0	92	1180	0.31	217	4.55×10^{-5}	1.8	2.8	0.33	67.5
8.0	92	2360	0.31	217	4.55×10^{-5}	1.9	1.1	0.03	165.2

Table 1: Flow parameters for which iLES was performed.

3. Acoustic Models

3.1. Lowson - 1968

Lowson [4] has derived one of the first empirical expressions for estimating the power spectral density beneath an attached supersonic turbulent

boundary layer. Based on subsonic and supersonic wind tunnel experimental results, the model is formulated as

$$\frac{\Phi(\omega)U_\infty}{P'^2_{rms}\delta} = \frac{1.0}{8.0\left(1+\left(\frac{\omega}{\omega_0}\right)^2\right)^{3/2}}, \tag{1}$$

where the typical frequency ω_0 is equal to $8U_\infty/\delta$. In addition to the spectral model, Lowson has proposed a simple semi-empirical equation for the pressure fluctuation intensity (P'_{rms})

$$P'_{rms} = \frac{0.006q_\infty}{1+0.14M^2}, \tag{2}$$

where $q_\infty = \rho_\infty U_\infty^2/2$ is the dynamic pressure.

The use of Eq. 1 requires the knowledge of the boundary layer thickness (δ), which can either be measured from experiments, calculated from numerical simulations or predicted by empirical formulas like the one suggested by Bies [23]

$$\delta = 0.37xRe_x^{-0.2}\left[1+\left(\frac{Re_x}{6.9\times10^7}\right)^2\right]^{0.1}, \tag{3}$$

where x is the distance from the leading edge of the body to the point of interest and $Re_x = U_\infty x/\nu_\infty$. Empirical formulas based on free stream conditions are used in all the cases presented in this paper, unless otherwise stated.

Robertson [24] showed that Lowson's model underestimates the wall pressure spectral density at low frequencies, a behaviour that was not found in the present compressible simulations (Figure 1). The model has a good overall agreement with the iLES spectra in the low and mid frequency regions. Significant deviations are observed in the high frequency region, particularly at hypersonic Mach numbers. The discrepancies at high frequencies may be due to a number of factors, including sensors resolution (experiment), as well as the fact that the model has been designed using subsonic and supersonic experimental data. Compressibility effects in the hypersonic Mach range have not been taken into account.

3.2. Maestrello - 1969

Maestrello [5] performed measurements on the side wall of a supersonic wind tunnel and developed a semi-empirical wall pressure spectrum model.

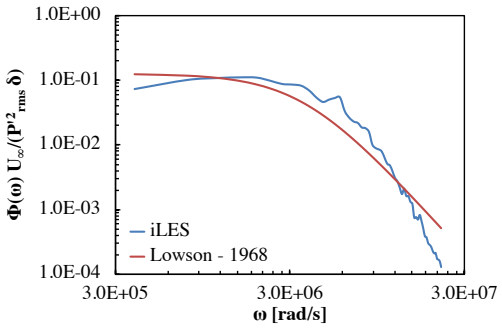

(a) M = 2.25

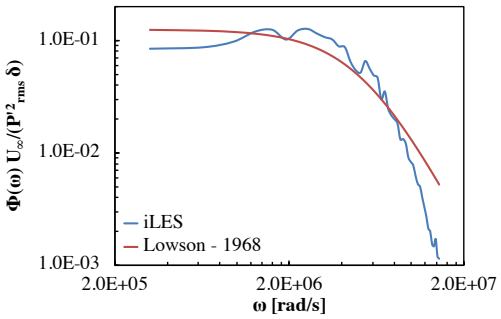

(b) M = 4.0

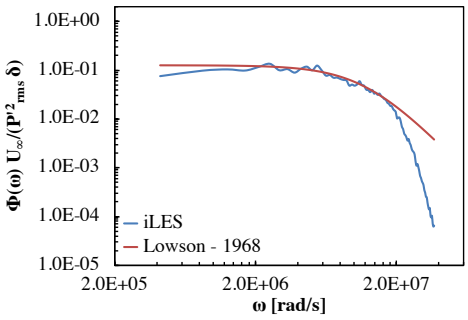

(c) M = 8.0

Figure 1: Comparison of Lowson's model with the iLES spectra beneath supersonic and hypersonic TBLs.

The pressure data included measurements in the range between 0.8 to 200 kHz and at Mach numbers of 1.42, 1.98, 2.99 and 3.98. Maestrello's model is given by

$$\Phi(\omega)U_\infty/(P'^2_{rms}\delta) = \sum_{n=1}^{4} A_n e^{-K_n(\omega\delta/U_\infty)}, \tag{4}$$

where

$$\begin{aligned} A_1 &= 0.044, \quad K_1 = 0.0578, \\ A_2 &= 0.075, \quad K_2 = 0.243, \\ A_3 &= -0.093, \quad K_3 = 1.12, \\ A_4 &= -0.025, \quad K_4 = 11.57. \end{aligned} \tag{5}$$

The above constants determine the spectral peak value, which occurs at $\omega\delta/U_\infty \sim 1.5$, and also control the rate of roll-off from the peak. The bound-

ary layer thickness δ is calculated by the empirical formula suggested by Bies [23] (Eq. 3).

Maestrello's model gives satisfactory results in the low frequency spectrum of the wall pressure fluctuations but fails to predict the roll-off rate in the high frequency regime (Figure 2). This can also be explained by the upper frequency limit of the experimental measurements that the model was based on. A major advantage of this model is its simplicity and minimal amount of input information needed, namely the free-stream velocity of the flow and the boundary layer thickness.

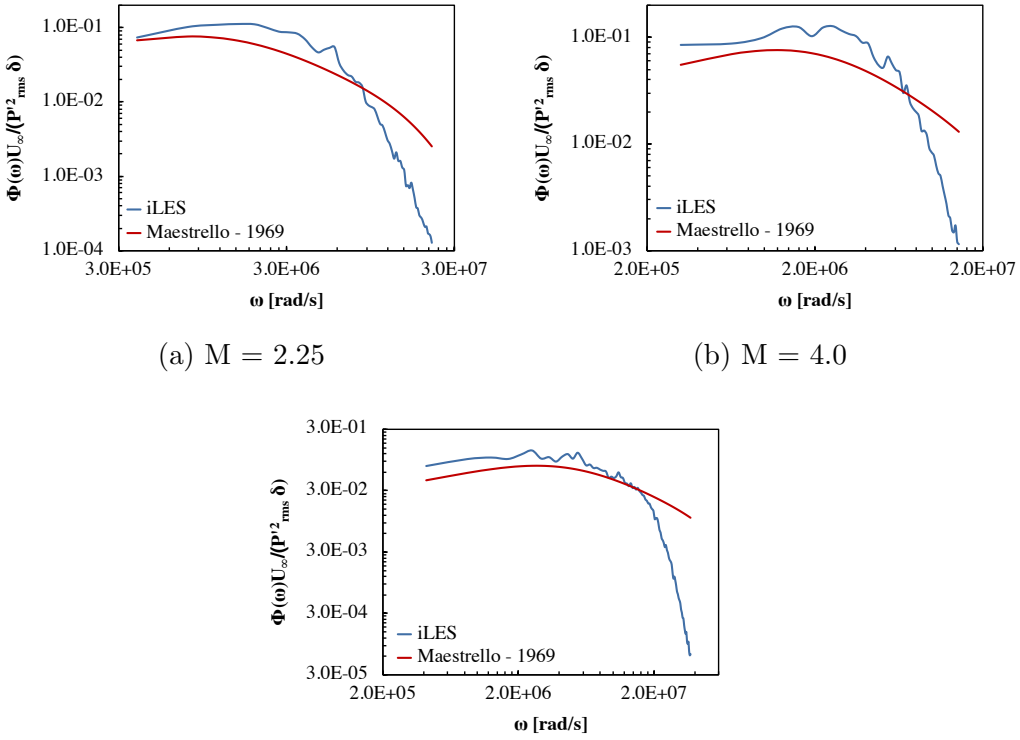

(a) M = 2.25

(b) M = 4.0

(c) M = 8.0

Figure 2: Comparison of Maestrello's model with the iLES spectra beneath supersonic and hypersonic TBLs.

3.3. Robertson - 1971

Robertson [24] extended Lowson's work [4] using subsonic and supersonic wind tunnel measurements. He proposed a model with small modifications

targeted to improve the high-frequency roll-off, and increase the spectrum amplitude at low frequencies. The dimensionless form of Robertson's model for the wall pressure spectrum is given by

$$\frac{\Phi(\omega)U_\infty}{P'^2_{rms}\delta^*} = \frac{1.0}{0.5\left(1+\left(\frac{\omega}{\omega_0}\right)^{0.9}\right)^2}, \tag{6}$$

where the displacement thickness δ^* is used in the calculation of ω_0, with $\omega_0 = U_\infty/(2\delta^*)$. For the calculation of the displacement thickness an empirical equation is used

$$\delta^* = \frac{\delta(1.3+0.43M^2)}{10.4+0.5M^2\left(1+2\times10^{-8}Re_x\right)^{1/3}}, \tag{7}$$

where the boundary layer thickness is calculated by Eq. 3.

The changes suggested by Robertson [24] do not improve Lowson's models, thus the spectrum roll-off is not captured (Figure 3). Note the measurements were based on subsonic and supersonic flows and not on hypersonic flows.

3.4. Cockburn & Robertson - 1974

Cockburn and Robertson [25] modified Lowson's model in connection with the vibration response of spacecraft shrouds to in-flight fluctuating pressures. The model was formulated in terms of the outer variable scaling, and focused at the frequency spectrum of wall pressures at transonic and supersonic speeds. The model is similar to the one proposed by Robertson [24] and has the following form:

$$\frac{\Phi(f)U_\infty}{q^2_\infty\delta} = \frac{P'^2_{rms}/q^2_\infty}{(\delta f_0/U_\infty)[1+(f/f_0)^{0.9}]^2}, \tag{8}$$

where the mean square pressure fluctuations are calculated by Eq. 2; f is the frequency; and f_0 the characteristic frequency $f_0 = 0.346U_\infty/\delta$. The predicted spectrum has a maximum at zero frequency and drops off faster when frequencies exceed the characteristic f_0. At high frequencies the model varies as $\omega^{-1.8}$, which is quite different from the spectral characteristics of wall pressure fluctuations predicted by iLES (Figure 4) and by previous DNS[26, 27], theoretical[28, 29] and experimental studies[30, 31]. The low frequency content of the spectrum is captured for all Mach numbers, but the spectrum roll-off deviates from the iLES results.

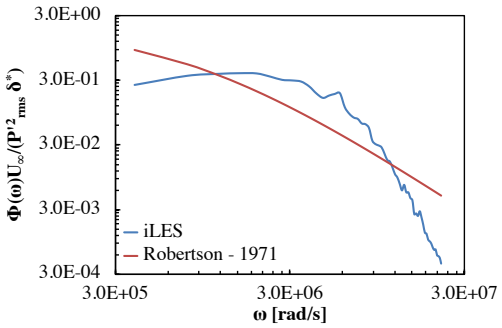

(a) M = 2.25

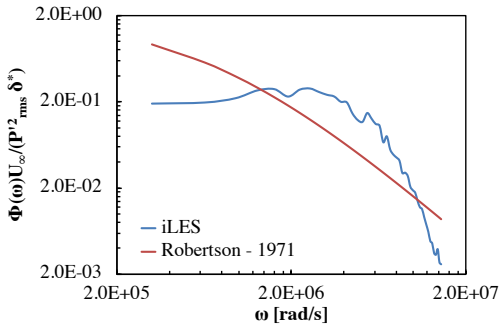

(b) M = 4.0

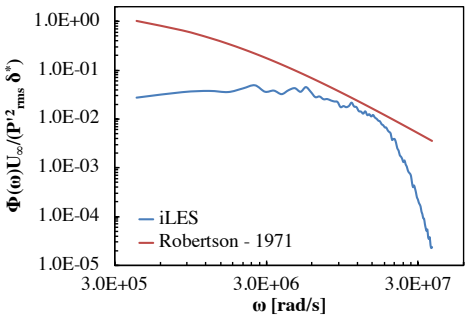

(c) M = 8.0

Figure 3: Comparison of Robertson's model with the iLES spectra beneath supersonic and hypersonic TBLs.

3.5. Amiet - 1976

Amiet [1] proposed a model for trailing edge noise based on measurements over a flat plate [32]. Amiet related the far-field acoustic signature statistics to the aerodynamic wall pressure statistics at some point upstream of the trailing edge. According to Amiet's model the wall pressure fluctuations are utilised as an equivalent acoustic source. The proposed model for the spectrum beneath a turbulent boundary layer is valid only in a region of the frequency spectrum, $0.1 < \bar{\omega} = \omega\delta^*/U_\infty < 20$, and is written as

$$\frac{\Phi(\omega)U_\infty}{q_\infty^2\delta^*} = \frac{2\times10^{-5}}{1+\bar{\omega}+0.217\bar{\omega}^2+0.00562\bar{\omega}^4}. \tag{9}$$

Amiet's model over-estimates the spectrum amplitude in the low frequency regime (Figure 5) and the high frequency slope is not steep enough. The

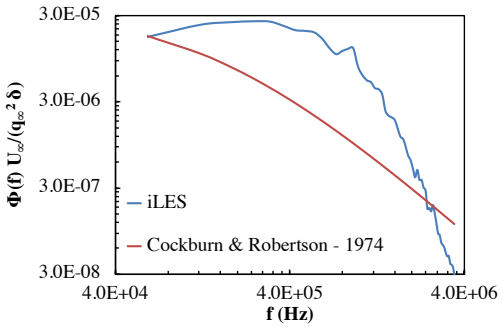

(a) M = 2.25

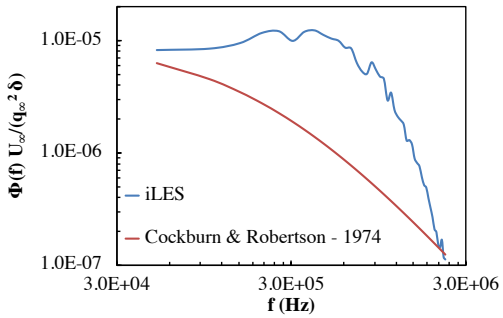

(b) M = 4.0

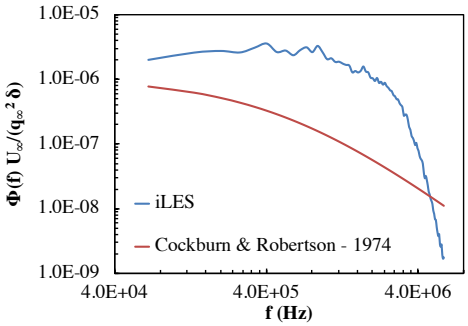

(c) M = 8.0

Figure 4: Comparison of Cockburn and Robinson's model with the iLES spectra beneath supersonic and hypersonic TBLs.

mid-frequency region is captured quite well in terms of the amplitude and the roll-off slope. Amiet's model has similar restrictions as the models presented above, where sensor resolution and compressibility effects can significantly affect the accuracy of a model, especially in high-speed flows as those presented in this paper.

3.6. Efimtsov - 1982

Efimtsov [33, 34, 35, 36] used wind tunnel experiments and flight data in order to develop two models. The data that formed the basis of the first model covers a range of subsonic and supersonic Mach numbers ($0.41 < M < 2.1$), as well as Reynolds numbers ($5 \times 10^7 < Re_x < 4.85 \times 10^8$). For the second model, which is the one considered here, the range of applicability was extended by further collecting wind tunnel and flight data for Mach

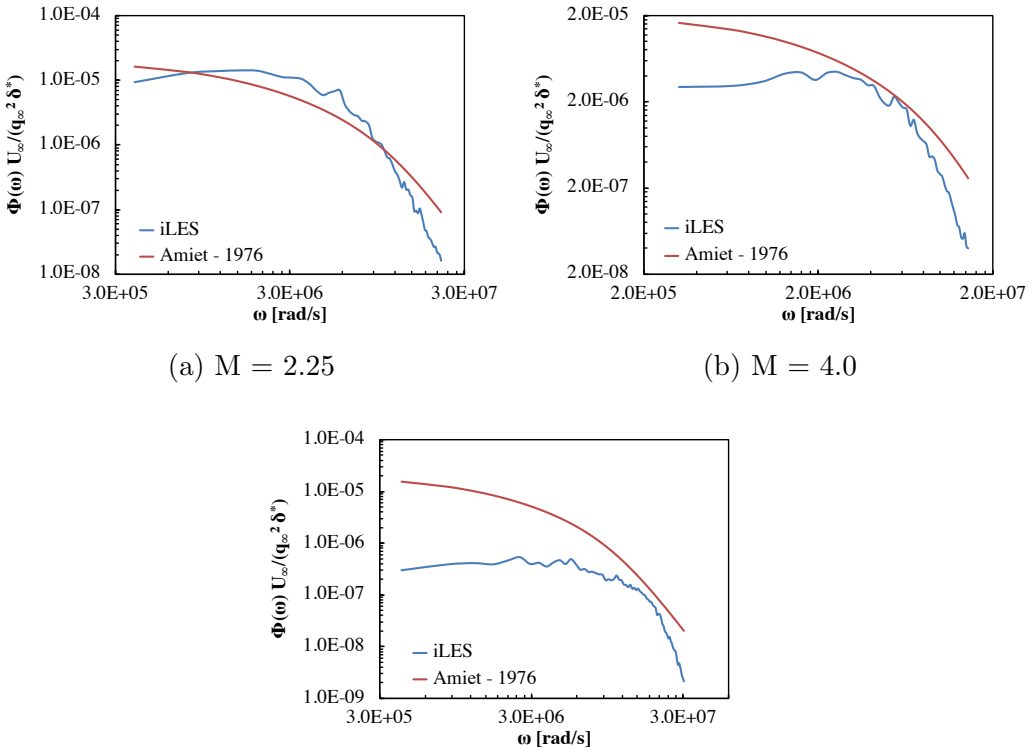

(a) M = 2.25

(b) M = 4.0

(c) M = 8.0

Figure 5: Comparison of Amiet's model with the iLES spectra beneath supersonic and hypersonic TBLs.

numbers from 0.05 to 2.5 and the full practical range of Re_x. The second semi-empirical model proposed by Efimtsov [35, 36] is given by

$$\frac{\Phi(\omega)}{\rho_\infty^2 u_\tau^3 \delta} = \frac{\alpha\beta}{(1+8\alpha^3 Sh^2)^{1/3} + \alpha\beta Re_\tau \left(\frac{Sh}{Re_\tau}\right)^{10/3}}, \tag{10}$$

where $\alpha = 0.01$; $\beta = \left[1 + \left(\frac{Re_{\tau 0}}{Re_\tau}\right)^3\right]^{1/3}$; $Sh = \omega\delta/u_\tau$; $u_\tau = U_\infty\sqrt{0.5C_f}$, $Re_\tau = \frac{\delta u_\tau}{\nu_w}$; and $Re_{\tau 0} = \frac{\delta u_\tau}{\nu_\infty}$. Efimtsov's model also includes a variable that takes into account compressibility effects. The friction Reynolds number Re_τ requires the viscosity of the fluid near the wall (ν_w), which can be estimated

through the following equation,

$$\nu_w = \nu_\infty \frac{\rho}{\rho_w} \left(\frac{T_w}{T_\infty} \right)^r, \tag{11}$$

where $r = 0.896$ is the adiabatic wall recovery factor. The near-wall density and temperature are defined by $\rho_w = \rho_\infty T_\infty / T_w$ and $T_w = T_\infty \left[1 + \frac{r(\gamma-1)}{2} M^2 \right]$, respectively, where $\gamma = 1.4$ is the ratio of specific heats for air. Eq. 10 requires the knowledge of the coefficient of friction (C_f), which can be obtained from the relation proposed by Schultz-Grunov[37],

$$C_f = 0.37(log_{10} Re_x)^{-2.584}. \tag{12}$$

Efimtsov's model produces a spectrum that scales with $\omega^{-10/3}$ at the high-frequency limit. Figure 6 compares the spectra of Efimtsov's model with the iLES data. The model reproduces the correct shape of the spectrum roll-off for the supersonic Mach number, but it over-predicts the amplitude in the low and high frequency regions. At higher Mach numbers, which lay outside the applicability range of the model, the over-prediction at the low-frequency limit is several orders of magnitude and the overall spectrum shape is not reproduced correctly.

3.7. Chase - 1987

Chase [38] presented a comprehensive semi-empirical model for an incompressible fluid based on Kraichnan's results [39]. The model was further improved in a follow-up paper [6] through the inclusion of fluid compressibility. The most recent version of Chase's model [6, 40] is given by

$$\frac{\Phi(\omega)}{\rho_\infty^2 u_\tau^3 \delta} = \frac{u_\tau [a_+ \gamma_M \alpha^{-3} (1 + \mu_M^2 \alpha^2) + 3\pi C_T \alpha^{-1} (1 + \alpha^{-2})]}{\delta \omega}, \tag{13}$$

where $\alpha^2 = 1 + (b\omega\delta/U_c)^{-2}$; $C_M = 0.1553$, $C_T = 0.00467$, $b = 0.75$, $\mu_M = 0.176$, $a_+ = 2\pi(C_M + C_T)$; $\gamma_M = C_M/(C_M + C_T)$; and $U_c = 3u_\tau/\mu_M$. This model has been designed to produce a spectrum with scaling ω^0 at the low-frequency limit and ω^{-1} at high frequencies. The model cannot decay faster than ω^{-1} and has limited applicability to low and medium frequencies. Figure 7 shows that the model produces values much higher than the iLES across a range of frequencies.

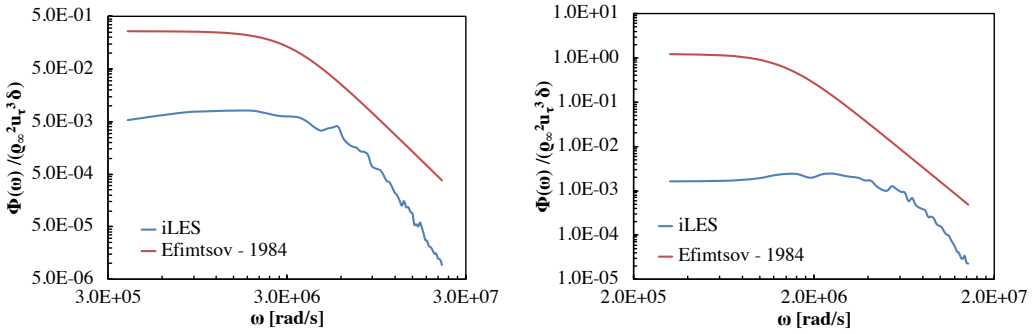

(a) M = 2.25 (b) M = 4.0

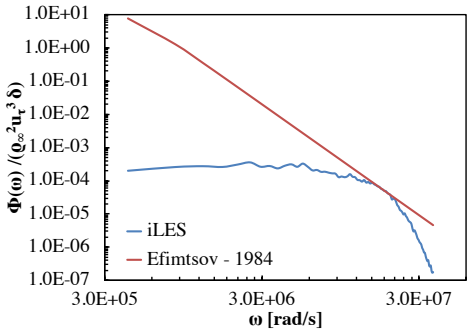

(c) M = 8.0

Figure 6: Comparison of Efimtsov's model with the iLES spectra beneath supersonic and hypersonic TBLs.

3.8. Laganelli & Wolfe - 1989

Laganelli and Wolfe [7] proposed a model based on Robertson's work [24] that takes into account viscous effects, compressibility and heat transfer of the medium. Both experimental data and fluid dynamics principles of attached zero-pressure gradient and separated turbulent boundary layer flows were taken into account during the development of this model. The proposed model depends on the friction coefficient F_C and is defined as:

$$\frac{\Phi(\omega)U\infty}{q_\infty^2\delta^*} = 2.293\frac{10^{-5}F_C^{-0.5733}}{1+F_C^{2.867}\left(\frac{\delta^*}{U_\infty}\omega\right)^2}, \tag{14}$$

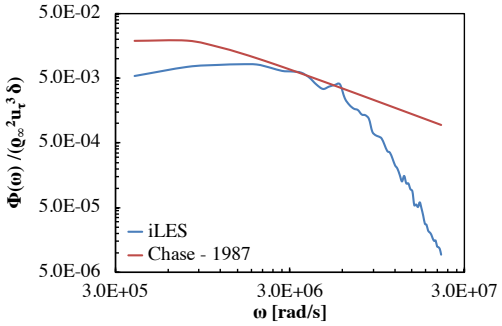

(a) M = 2.25

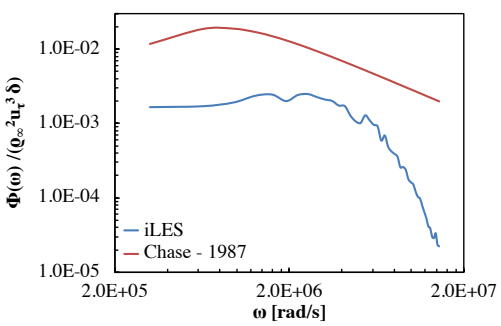

(b) M = 4.0

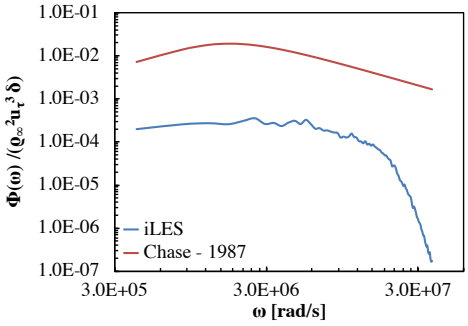

(c) M = 8.0

Figure 7: Comparison of Chase's model with the iLES spectra beneath supersonic and hypersonic TBLs.

where F_C accounts for the compressibility and heat transfer properties of the medium through the formula:

$$F_C = \frac{1}{2} + \frac{h_w}{h_{aw}}\left(\frac{1}{2} + r\frac{\gamma-1}{2}M^2\right) + 0.22r\frac{\gamma-1}{2}M^2, \tag{15}$$

where h_w/h_{aw} is the ratio of specific enthalpy between normal and adiabatic wall conditions.

The proposed compressibility corrections work for weakly compressible flows but do not provide satisfactory results for the supersonic and hypersonic flows considered here (Figure 8). For the supersonic flow the model manages to capture the frequency amplitude at the very low frequency limit, but the spectrum roll-off is significantly steeper than the one calculated from the iLES results. The deviation from the iLES results is greater at higher Mach

numbers.

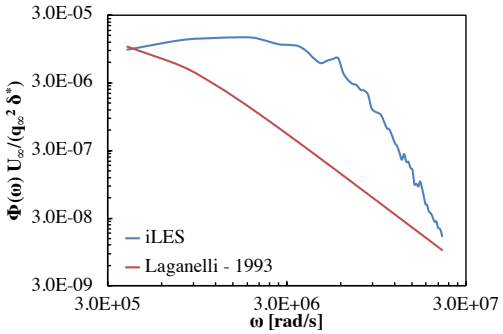

(a) M = 2.25

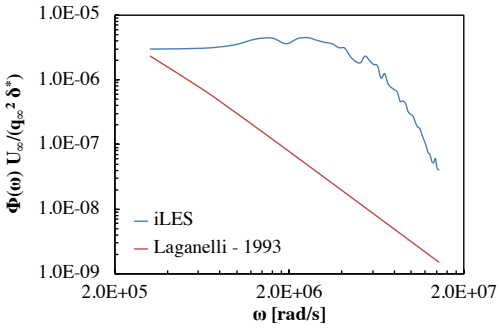

(b) M = 4.0

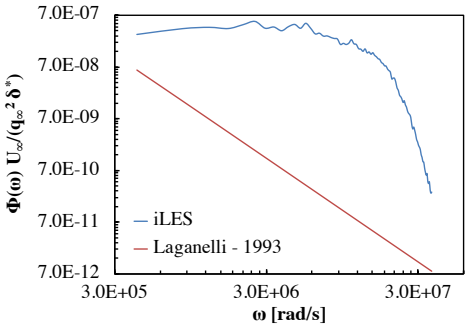

(c) M = 8.0

Figure 8: Comparison of Laganelli and Wolfe's model with the iLES spectra beneath supersonic and hypersonic TBLs.

3.9. Smol'yakov & Tkachenko - 1991

Smol'yakov and Tkachenko [41] proposed a model given by

$$\frac{\Phi(\omega)U\infty}{q_\infty^2\delta^*} = \frac{5.1C_f^2}{1+0.44(\omega\delta^*/U_\infty)^{7/3}}, \tag{16}$$

where the skin friction coefficient is calculated by Eq. 12.

This model produces a flat spectrum in the low and mid frequency regions, while for higher frequencies it decays as $\omega^{-7/3}$. The model over-predicts the magnitude of the pressure fluctuation for all Mach numbers and over the whole range of frequencies (Figure 9). The deviation from the iLES spectra

is significant in the low frequency region with an apparent trend to increase for higher Mach numbers. The discrepancies arise from the non-inclusion of fast-decaying (high) frequencies and compressibility effects.

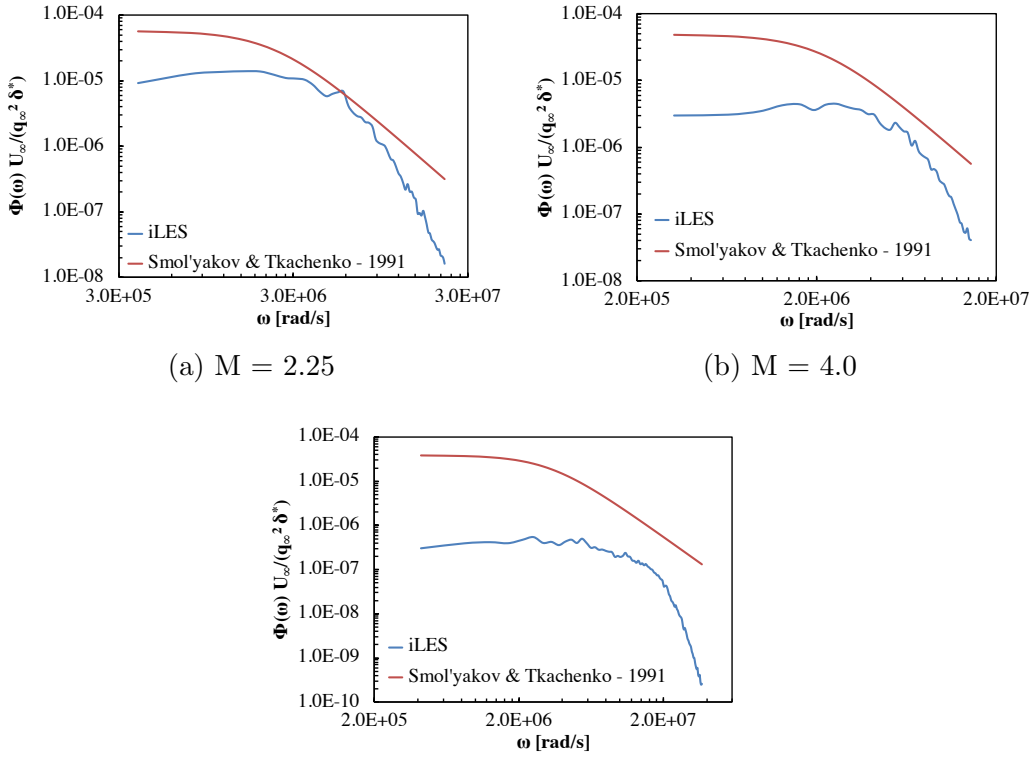

(a) M = 2.25 (b) M = 4.0

(c) M = 8.0

Figure 9: Comparison of Smol'yakov and Tkanchenko's model with the iLES spectra beneath supersonic and hypersonic TBLs.

3.10. Smol'yakov - 2000

Smol'yakov proposed a model based on several sets of experimental data from the literature[2]. This model comprises three different equations with different scaling variables in an effort to reproduce the frequency regions that have been established for pressure spectra beneath zero-pressure gradient, fully turbulent boundary layers [28, 29, 42]. Each equation is used in a range of dimensional frequency $\bar{\omega} = \omega\nu_\infty/u_\tau^2$, where the friction velocity u_τ can be calculated by the Falkner formula[2] for the friction coefficient

$$C_f = 2\tau_w/(\rho_\infty U_\infty^2) = 2(u_\tau/U_\infty)^2 = 0.0263 Re_x^{-1/7} \tag{17}$$

as proposed by Smol'yakov [2]. The model has been developed for $Re_\theta = U_\infty \theta/\nu_\infty > 1,000$, where θ is the momentum thickness of the boundary layer. The set of equations for the Smol'yakov's model is given by

$$\begin{aligned}
&\frac{\Phi(\omega)u_\tau^2}{\tau_w^2\nu_\infty} = 1.49\times10^{-5}R_\theta^{2.74}\bar{\omega}^2(1-0.117R_\theta^{0.44}\bar{\omega}^{0.5}) \\
&\qquad \text{when } \bar{\omega} < \bar{\omega}_0, \\
&\frac{\Phi(\omega)u_\tau^2}{\tau_w^2\nu_\infty} = 2.75\bar{\omega}^{-1.11}\left\{1-0.82\exp\left[-0.51(\bar{\omega}/\bar{\omega}_0-1)\right]\right\} \\
&\qquad \text{when } \bar{\omega}_0 < \bar{\omega} < 0.2, \\
&\frac{\Phi(\omega)u_\tau^2}{\tau_w^2\nu_\infty} = (38.9e^{-8.35\bar{\omega}} + 18.6e^{-3.58\bar{\omega}} + 0.31e^{-2.14\bar{\omega}}) \\
&\qquad \times\left\{1-0.82\exp\left[-0.51(\bar{\omega}/\bar{\omega}_0-1)\right]\right\} \\
&\qquad \text{when } \bar{\omega}_0 < \bar{\omega} < 0.2,
\end{aligned} \tag{18}$$

where $\bar{\omega}_0 = 49.35R_\theta^{-0.88}$. The momentum thickness is calculated by the formula proposed by Bies [23]

$$\theta = \frac{\delta}{10.4 + 0.5M^2[1+2\times10^{-8}Re_x]^{1/3}}. \tag{19}$$

The spectrum produced by Eq. 18 is proportional to ω^2 in the low-frequency region, $\bar{\omega} < \bar{\omega}_0$. The model gives a peak value in the mid-frequency region, followed by spectra $\omega^{-1.11}$ in the universal region $\bar{\omega}_0 < \bar{\omega} < 0.2$. In the high-frequency region, $\bar{\omega}_0 < \bar{\omega} < 0.2$, the produced spectrum varies by an exponent value rather than a power-law form. However, the various parts of the exponent can be approximated by power-law dependence ω^{-k}, where k takes a larger value when increasing frequency.

This model has been developed through a thorough analysis of the available theory and experimental data. Compressibility effects have not been considered either in the model formulation or in the sub-models used to predict the friction velocity and momentum thickness. As a result, the predicted spectra deviate from the iLES ones as the Mach number increases (Figure 10). This model has the potential to produce better spectrum predictions with small adjustments and can be used in its current form for flows at $M < 2.0$, for rough order of magnitude estimations, and with higher accuracy for $M < 1.0$.

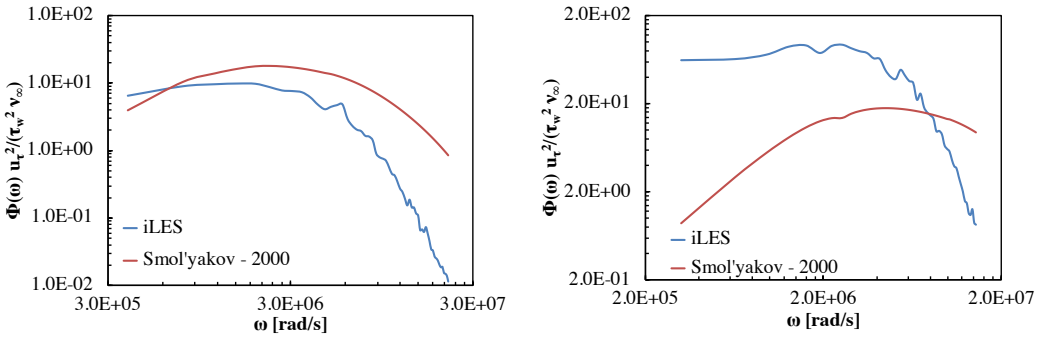

(a) M = 2.25 (b) M = 4.0

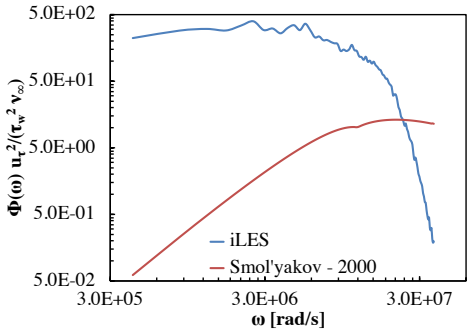

(c) M = 8.0

Figure 10: Comparison of Smol'yakov's model with the iLES spectra beneath supersonic and hypersonic TBLs.

3.11. Goody - 2004

Goody [3] proposed a model that produces a scaling behaviour similar to Smol'yakov's model, which is the theoretically, numerically and experimentally established pressure spectrum scaling for zero-gradient, fully turbulent subsonic and supersonic flows. Goody's model consists of one equation, based on Howe's work [43] and data sets from various experimental studies [44, 31, 30, 45, 46, 47, 48]:

$$\frac{\Phi(\omega)U_\infty}{\tau_w^2\delta} = \frac{C_2(\omega\delta/U_\infty)^2}{[(\omega\delta/U_\infty)^{0.75}+C_1]^{3.7}+[C_3R_T^{-0.57}(\omega\delta/U_\infty)]^7}, \tag{20}$$

where $C_1 = 0.5$, $C_2 = 3.0$ and $C_3 = 1.1$ are empirical constants, and $R_T = (\delta/u_\infty)/(\nu_\infty/u_\tau^2)$ is the ratio of the outer to inner boundary layer time scale. The Reynolds number effect on the overlap region of the spectrum is

introduced through the ratio C_1 over $C_3 R_T^{-0.57}$, which determines the size of the predicted overlap region.

Goody's model gives good predictions when compared to both numerical and experimental data over a range of Reynolds and Mach numbers [40, 8, 9]. Figure 11 shows that Goody's model reproduces correctly the pressure spectrum from low up to high frequencies, including the overlap region across a range of Mach numbers. The over-prediction in the high-frequency region is due to compressibility effects that have not been incorporated in the model. Modifications of the model to address this issue are discussed in the next section.

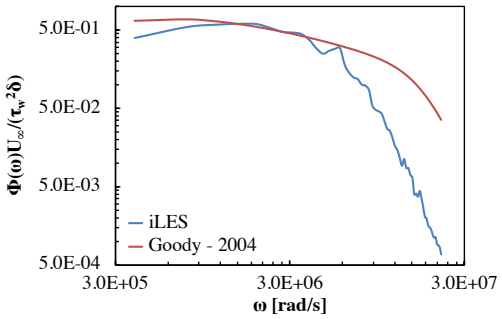

(a) M = 2.25

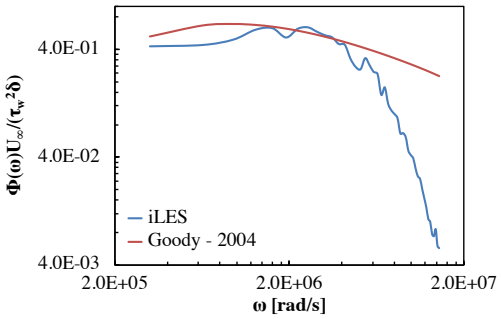

(b) M = 4.0

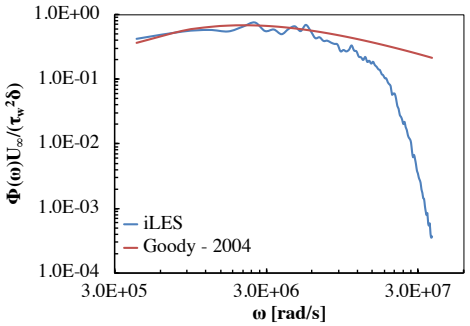

(c) M = 8.0

Figure 11: Comparison of Goody's model with the iLES spectra beneath supersonic and hypersonic TBLs.

3.12. Hu - 2016

Hu and Herr [8] performed a series of wind-tunnel experiments of zero, as well as favourable and adverse pressure gradient TBL. They developed a model based on Goody's formula (Eq. 20) in conjunction with new scaling variables and with reference to the adverse pressure gradient measurements:

$$\frac{\Phi(\omega)u_\tau}{q_\infty^2\theta} = \frac{a(\omega\theta/U_\infty)^b}{[(\omega\theta/U_\infty)^c + d]^e + [f(\omega\theta/U_\infty)]^g}, \tag{21}$$

where all the values of the constants are summarised in table 2.

$a = (81.004d + 2.154) \times 10^{-7}$	$b = 1.0$
$c = 1.5h^{1.6}$	$d = 10^{-5.8\times10^{-5}Re_\theta H - 0.35}$
$e = 1.13/h^{0.6}$	$f = 7.645Re_\tau^{-0.411}$
$g = 6$	$h = 1.169\ln(H) + 0.642$

Table 2: Model constants for Eq. 21. $H = \delta^*/\theta$ is the shape factor.

The iLES results we compare against the models are from zero-pressure gradient simulations, thus a model that has been designed for adverse pressure gradient flows is not expected to give accurate results. Figure 12 compares the present iLES with Hu's and Herr's model predictions. The model gives relatively good results in the supersonic flow. However, for higher Mach numbers the predictions deviate significantly either in the low-frequency region, for the $M = 4$ flow, or in the high frequency region for the $M = 8$ flow case.

3.13. Lee - 2018

Lee's [9] model was validated against experimental data from the literature for zero and adverse pressure gradient flows. Lee also assessed five recent models proposed by other authors and concluded that the models proposed by Goody [3] and Hu & Herr [8] are the most accurate ones for zero pressure gradient flows. To extend the applicability of his model, he used Rozenberg's model [49] and extended it to zero pressure gradient flows, non-symmetric and high-loading airfoil flows. The new model was calibrated for flows in the range of $1.4 \times 10^3 \leq Re_\theta \leq 2.34 \times 10^4$ and frequencies between 100 and $10,000$ Hz. Lee's model is given by

$$\frac{\Phi(\omega)U_\infty}{\tau_w^2\delta^*} = \frac{max(a, (0.25\beta_c - 0.52)a)(\omega\delta^*/U_\infty)^2}{[4.76(\omega\delta^*/U_\infty)^{0.75} + d^*]^e + [8.8R_T^{-0.57}(\omega\delta^*/U_\infty)]^{h^*}}, \tag{22}$$

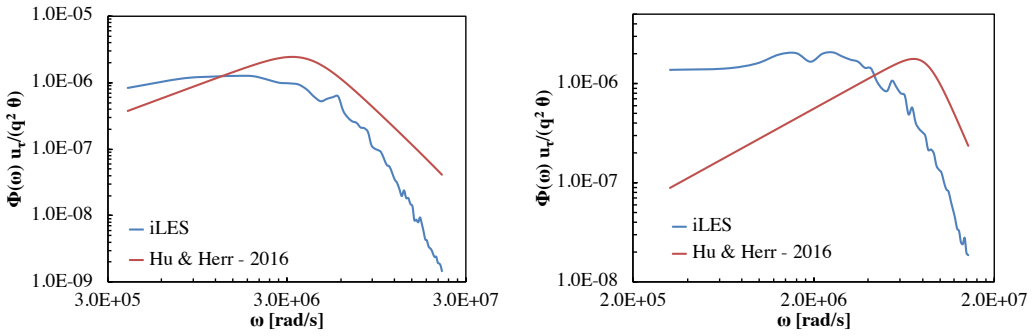

(a) M = 2.25 (b) M = 4.0

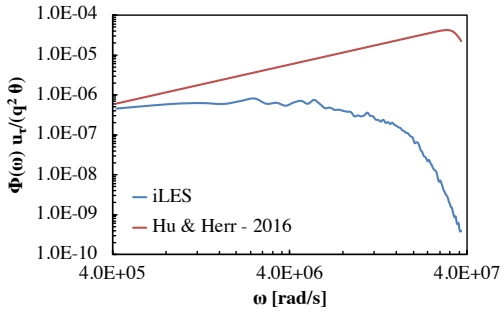

(c) M = 8.0

Figure 12: Comparison of Hu's and Herr's model with the iLES spectra beneath supersonic and hypersonic TBLs.

where $\beta_c = (\theta/\tau_w)(dp/dx)$, $a = 2.82\Delta^2(6.13\Delta^{-0.75} + d)^e[4.2(\Pi/\Delta) + 1]$, $\Delta = \delta/\delta^*$, $\Pi = 0.8(\beta_c + 0.5)^{3/4}$, $d = 4.76(1.4/\Delta)^{0.75}[0.375e - 1]$ and $e = 3.7 + 1.5\beta_c$. The parameter h^* is defined as

$$h^* = min(3, (0.139 + 3.1043\beta_c)) + 7, \tag{23}$$

and the parameter $d^* = max(1.0, 1.5d)$ if $\beta_c < 0.5$.

This model has a consistent behaviour producing spectra with the correct shape but over-predicting the amplitude over the entire range of frequencies (Figure 13). There are two possible explanations for this behaviour. Firstly, the frequency range of the present iLES is outside the validated range of the model. Secondly, and more importantly, the compressibility effects have not been taken into account. According to Lee, the model may not be limited to low speed or incompressible flows but he also recognised that further

validation is needed for high-speed flows.

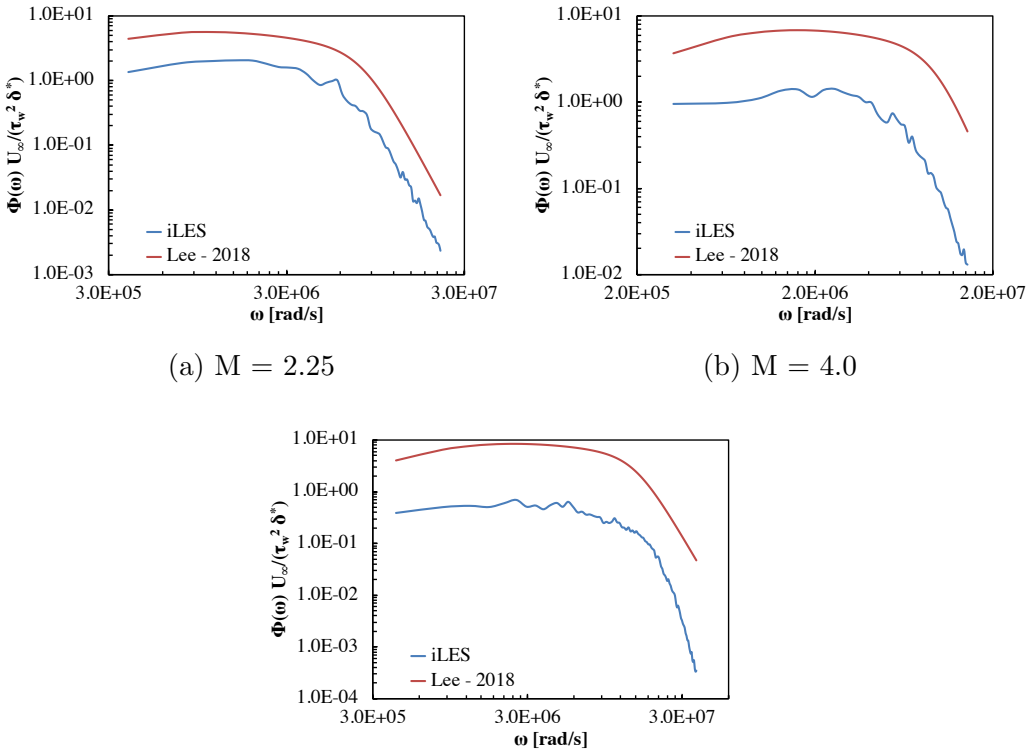

(a) M = 2.25 (b) M = 4.0

(c) M = 8.0

Figure 13: Comparison of Lee's model with the iLES spectra beneath supersonic and hypersonic TBLs.

4. Compressibility effects

In the previous sections, it was shown that existing models cannot accurately predict the pressure fluctuations spectrum beneath a zero-pressure gradient TBL in supersonic and hypersonic flows. The assumption of incompressibility adopted in the development of the aforementioned models has adversely affected the models' prediction. For example, Smol'yakov and Goody's models and the improvements suggested by Hu and Lee assume $\rho_\infty = \rho_w$ in the estimation of the friction velocity. For high-speed compressible flows the calculation of the skin friction velocity should be calculated by

$$u_\tau = \sqrt{\frac{\tau_w}{\rho_w}} = U_\infty \sqrt{\frac{1}{2} C_f \frac{\rho_\infty}{\rho_w}} \tag{24}$$

The ratio of the outer-layer to inner-layer timescale, R_T, proposed by Goody [3] for compressible flows yields

$$R_T = \frac{\delta/U_\infty}{\nu_w/u_\tau^2} = \frac{\delta u_\tau^2}{U_\infty \nu_w} = \frac{\delta u_\tau}{\nu_w} \sqrt{\frac{1}{2} C_f \frac{\rho_\infty}{\rho_w}} = U_\infty C_f \frac{\delta \rho_\infty}{2 \nu_w \rho_w}. \tag{25}$$

We will show below that using Eqs. 24 and 25 the produced spectrum is significantly improved, particularly in the high-frequency region of the spectrum. The effects of compressibility have been examined in relation to Efimtsov's and Goody's models; the modified models are henceforth labelled as COMPRA-E and COMPRA-G standing for compressible-acoustic-Efimtsov and compressible-acoustic-Goody, respectively. Substituting

$$u_\tau = U_\infty \sqrt{0.01315 Re_x^{-1/7} \rho_\infty / \rho_w} \tag{26}$$

into Eq. 10 yields

$$\frac{\Phi(\omega)}{\rho_\infty^2 u_\tau^3 \delta} = \frac{C_R \alpha \beta}{(1 + 8\alpha^3 Sh^2)^{1/3} + \alpha \beta Re_\tau \left(\frac{Sh}{Re_\tau}\right)^5}, \tag{27}$$

where

$$C_R = \begin{cases} \left(\frac{1}{M}\right)^5, & \text{if } M > 1; \\ 1, & \text{otherwise;} \end{cases} \tag{28}$$

is a scaling factor, a heuristic approach for taking into account the Mach number effects in supersonic and hypersonic flows.

A comparison of the COMPRA-E model with the iLES data demonstrates that the compressibility corrections improve the results (Fig. 14). For the highest Mach number COMPRA-E over-estimates the amplitude of the low frequency pressure fluctuations and under-estimates the amplitude of the high frequency ones.

To validate the applicability of the COMPRA-E model in low-speed incompressible flows the results are also compared with the experimental measurements of zero pressure-gradient boundary layer flows by Hu & Herr [8] (Figure 15a). The proposed model satisfactorily captures the spectrum in

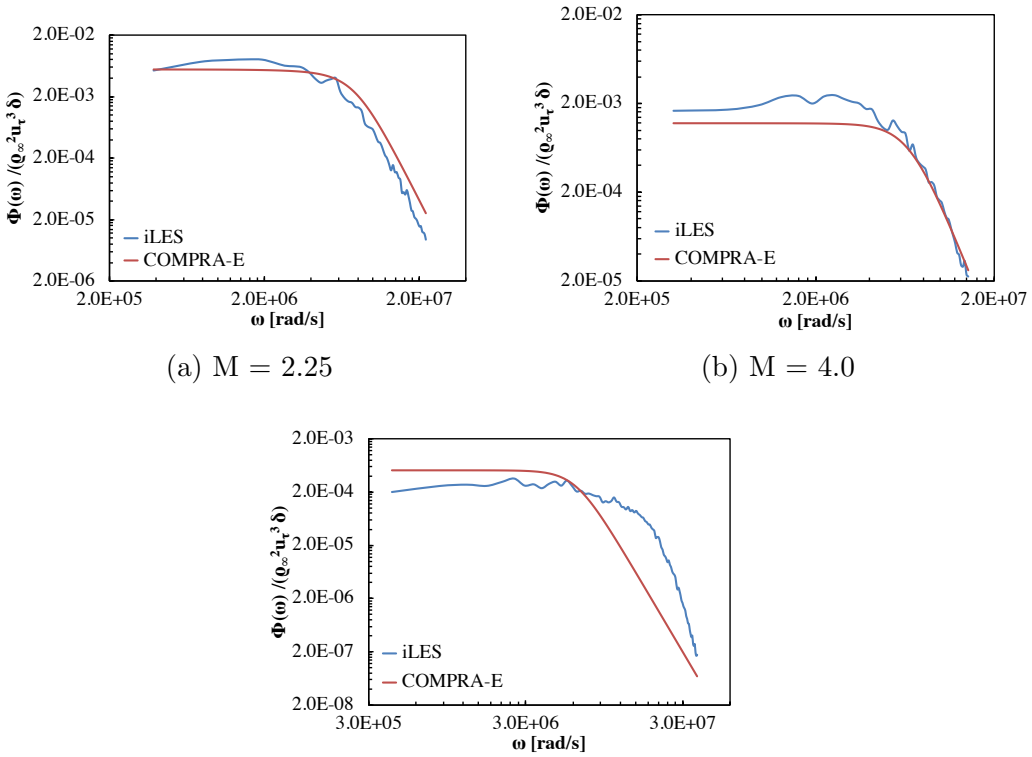

(a) M = 2.25

(b) M = 4.0

(c) M = 8.0

Figure 14: Comparison of the COMPRA-E model with iLES data. The original Efimtsov model predictions are not shown here because they would lie outside of the figure.

the overlap and high-frequency regions. However, in the low frequency region the shape of the predicted spectra do not match the experimentally measured ones.

In supersonic and hypersonic flows the results of COMPRA-E are also compared with the DNS of Duan et al. [26, 27]. Note that the spectrum for $M = 5.86$ has been compared with experimental measurements in [27] showing excellent agreement. Furthermore, the experimental and numerical data presented in Figure 15 have not been used for the calibration of the COMPRA-E or Efimtsov's models. All the parameters required for the calculation of the COMPRA-E model are given in Table 3. The COMPRA-E predictions deviate from the calculated spectra of the supersonic and hypersonic flows [26, 27]. The shape of the predicted spectrum is reproduced correctly but the amplitude is under-estimated with the deviations being larger

when increasing the Mach number (Figures 15b and 15c). Although the proposed scaling factor C_R provides an ad hoc improvement of the Efimtsov's model, it does not fully address the inaccuracy of the model in hypersonic flows.

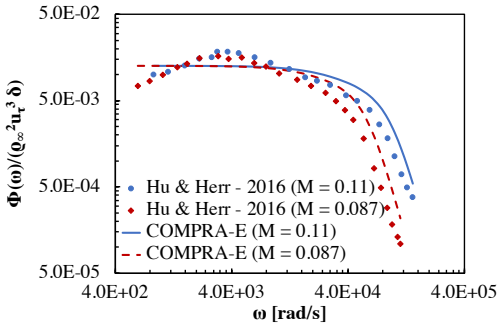

(a) Subsonic

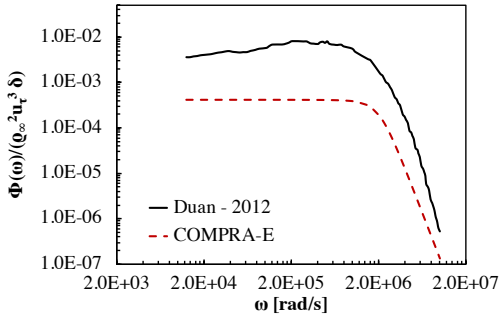

(b) Supersonic

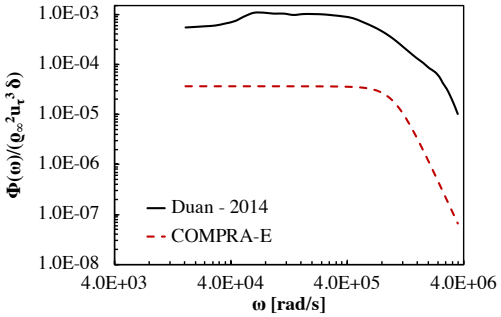

(c) Hypersonic

Figure 15: Validation of the COMPRA-E model with compressible and incompressible TBL experiments.

Ref.	M	$x(m)$	U_∞ (m/s)	ρ_∞ (kg/m^3)	T_∞ (K)	ν_∞ (m^2/s)
[8]	0.085	1.21	30.2	1.2	298	1.54×10^{-5}
[8]	0.11	1.21	39.2	1.2	298	1.54×10^{-5}
[26]	2.5	0.28	823.6	0.1	270	1.6938×10^{-4}
[27]	5.86	0.8	870.4	0.0427	54.97	8.727×10^{-5}

Table 3: Parameters used in the experiments and numerical simulations for the validation of the COMPRA-E and COMPRA-G models.

Goody's model was also investigated in conjunction with the compressibility corrections. Goody's model performs well in the low and medium frequency regions of the spectrum (Section 3.11), as well as overall in subsonic and supersonic zero-pressure gradient flows [3, 40, 8, 9]. The modified Goody's model (COMPRA-G) takes the following form:

$$\frac{\Phi(\omega)U_\infty}{\tau_w^2\delta} = \frac{C_2(\omega\delta/U_\infty)^2}{[(\omega\delta/U_\infty)^{0.75} + C_1]^{3.7} + [C_3 R_T^{C_{RG}}(\omega\delta/U_\infty)]^7}, \tag{29}$$

where the constants C_1 to C_3 are according to Goody [3];

$$C_{RG} = \begin{cases} -0.49, & \text{if } M > 1; \\ -0.57, & \text{otherwise;} \end{cases} \tag{30}$$

and R_T is obtained from Eq. 25. The compressibility corrections affect only the overlap and high-frequency regions of the predicted spectrum (Figure 16).

The COMPRA-G results are also compared with measurements and calculations from incompressible and compressible flows (Table 3). The model shows very good agreement with the experimental incompressible spectra of Hu & Herr [8] (Figure 17a). This result was expected as the original Goody's model has been thoroughly reviewed by Hu & Herr [8] showing an overall good agreement across a range of experimental measurements at zero pressure gradient.

COMPRA-G is also compared with the DNS of supersonic and hypersonic flows [26, 27] showing that the model provides satisfactory results for a range of Reynolds and Mach numbers.

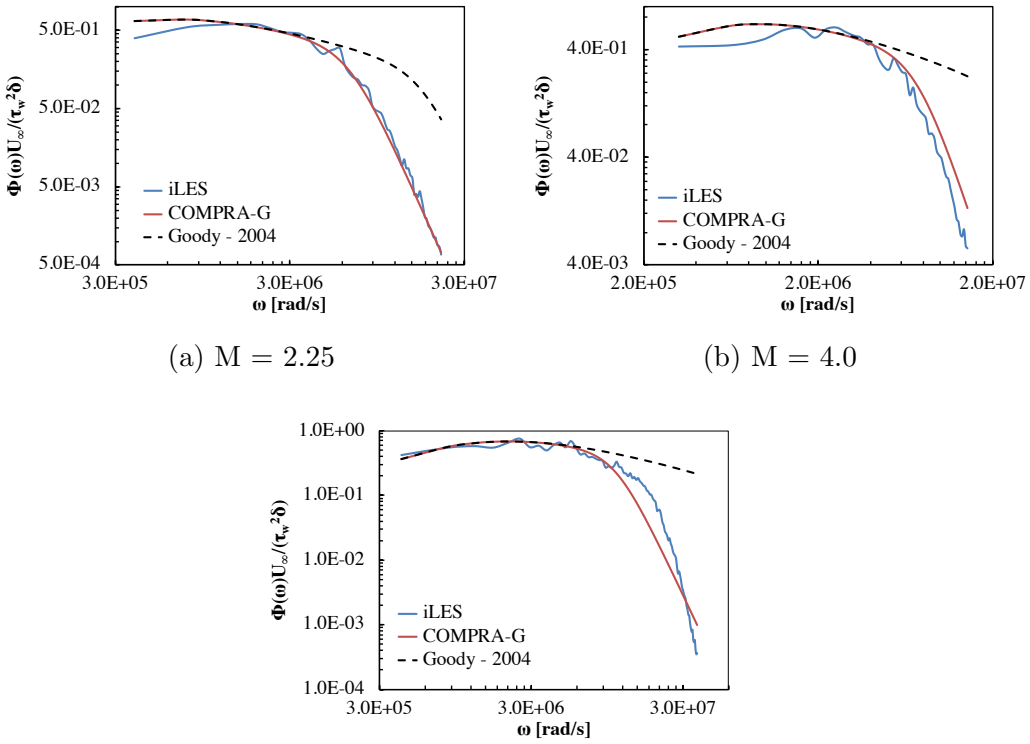

(a) M = 2.25

(b) M = 4.0

(c) M = 8.0

Figure 16: Comparison of the COMPRA-G model with compressible and incompressible TBL experiments.

5. Conclusions

Several spectra models for the pressure fluctuations beneath supersonic and hypersonic TBL have been investigated. The free-stream flow properties and the streamwise location have been used as input parameters for all the models. Boundary layer and near-wall properties have been estimated through correlations with the free-stream properties. The conclusions drawn from this study are summarised below:

- The existing models fail to capture the correct behaviour of pressure fluctuations in supersonic and hypersonic boundary layers across a broad range of frequencies.
- Compressibility corrections are required to improve the models' accuracy in supersonic and hypersonic flows.

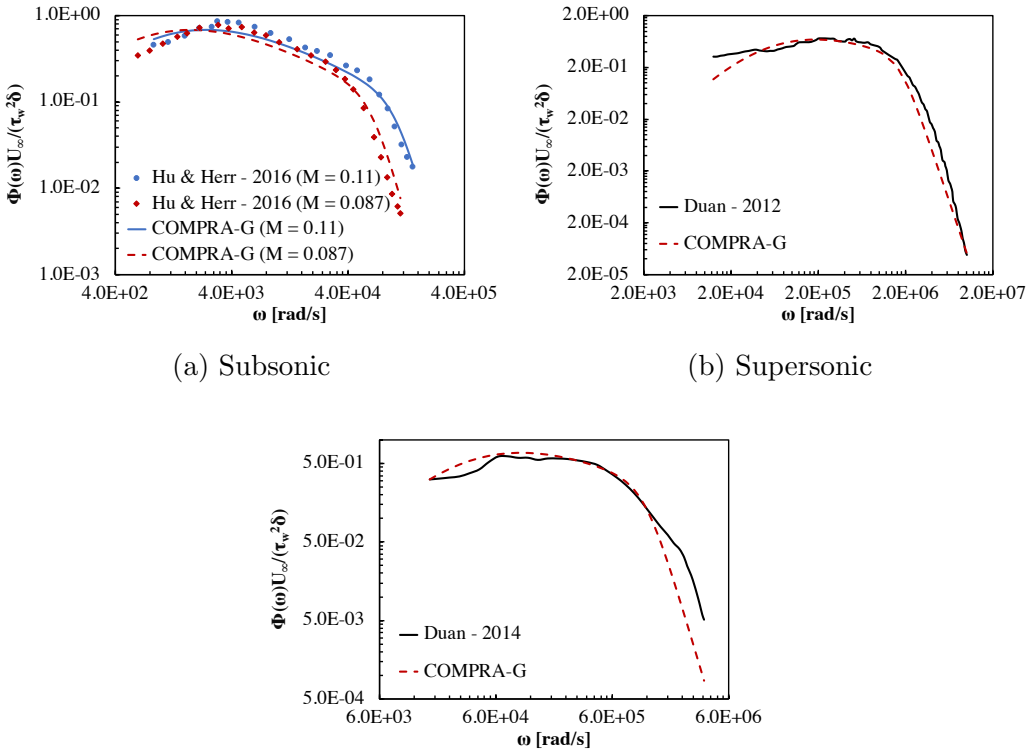

(a) Subsonic

(b) Supersonic

(c) Hypersonic

Figure 17: Validation of the COMPRA-G model with compressible and incompressible TBL.

- Goody's model gives satisfactory predictions of the low and medium frequency regions of the spectrum.
- Compressibility corrections have been proposed for Efimtsov's (COMPRA-E) and Goody's (COMPRA-G) models, which significantly improve the accuracy of the models in supersonic and hypersonic flows.
- The models have been validated against experimental and DNS data.
- The COMRPA-G model has shown very good agreement across a range of frequencies for zero pressure gradient supersonic and hypersonic flows.

Future studies will concern investigation of the modified models in high speed flows featuring adverse and favourable pressure gradient.

Acknowledgements

This work was sponsored by the Air Force Office of Scientific Research, Air Force Material Command, USAF, under grant number FA9550-14-1-0224. The U.S. Government is authorised to reproduce and distribute reprints for Governmental purpose notwithstanding any copyright notation thereon. The authors would like to thank S. M. Spottswood and Z. Riley at AFRL Structural Sciences Center, as well as D. Garner (EOARD) for their support. Results were obtained using the EPSRC funded ARCHIE-WeSt High Performance Computer (www.archie-west.ac.uk) under EPSRC grant no. EP/K000586/1.

[1] R. K. Amiet, Noise due to turbulent flow past a trailing edge, J. Sound Vib. 47 (3) (1976) 387–393.

[2] A. V. Smol'yakov, Calculation of the spectra of pseudosound wall-pressure fluctuations in turbulent boundary layers, Acoustical Physics 46 (3) (2000) 342–347.

[3] M. Goody, Empirical Spectral Model of Surface Pressure Fluctuations, AIAA Journal 42 (9) (2004) 1788–1794.

[4] M. V. Lowson, Prediction of boundary layer pressure fluctuations, Tech. rep., Air Force Flight Dynamics Laboratory (1968).

[5] L. Maestrello, Radiation from panel response to a supersonic turbulent boundary layer, J. Sound Vib. 10 (2) (1969) 261–295.

[6] D. M. Chase, The character of turbulent wall pressure spectrum at subconvective wavenumbers and a suggested comprehensive model, J. Sound Vib. 112 (1) (1987) 127–147.

[7] A. L. Laganelli, H. Wolfe, Prediction of fluctuating pressure in attached and separated tbl flow, in: AIAA 12th Aeroacoustics Conference, 1989.

[8] N. Hu, M. Herr, Characteristics of wall pressure fluctuations for a flat plate turbulent boundary layer with pressure gradients, in: 22nd AIAA/CEAS Aeroacoustics Conference, 2016.

[9] S. Lee, Empirical wall-pressure spectra modeling for zero and adverse pressure gradient flows, AIAA Journal.

[10] K. Ritos, I. W. Kokkinakis, D. Drikakis, S. M. Spottswood, Implicit large eddy simulation of acoustic loading in supersonic turbulent boundary layers, Phys. Fluids 29 (4) (2017) 1–11.

[11] K. Ritos, D. Drikakis, I. W. Kokkinakis, S. M. Spottswood, Acoustic loading in hypersonic transitional and turbulent boundary layers, J. Sound Vib. UNDER REVIEW.

[12] B. Thornber, D. Drikakis, Implicit Large-Eddy Simulation of a Deep Cavity Using High-Resolution Methods, AIAA Journal 46 (10) (2008) 2634–2645.

[13] B. Thornber, D. Drikakis, D. L. Youngs, R. J. R. Williams, The influence of initial conditions on turbulent mixing due to richtmyer-meshkov instability, J. Fluid Mech. 654 (2010) 99–139.

[14] Z. A. Rana, B. Thornber, D. Drikakis, Transverse jet injection into a supersonic turbulent cross-flow, Phys. Fluids 23 (046103) (2011) 1–21.

[15] K. Ritos, I. W. Kokkinakis, D. Drikakis, Physical insight into a mach 7.2 compression corner flow, in: AIAA Aerospace Sciences Meeting, Kissimmee, Florida, 2018.

[16] E. F. Toro, Riemann Solvers and Numerical Methods for Fluid Dynamics, 3rd Edition, Springer, 2009.

[17] D. S. Balsara, C. W. Shu, Monotonicity preserving weighted essentially non-oscillatory schemes with increasingly high order of accuracy, J. Comput. Phys. 160 (2) (2000) 405–452.

[18] D. Drikakis, W. Rider, High-Resolution Methods for Incompressible and Low-Speed Flows, Springer, 2005.

[19] F. Grinstein, L. Margolin, W. Rider, Implicit Large Eddy Simulation: Computing Turbulent Fluid Dynamics, Cambridge University Press, 2007.

[20] I. W. Kokkinakis, D. Drikakis, Implicit large eddy simulation of weakly-compressible turbulent channel flow, Comput. Method. Appl. M. 287 (2015) 229–261.

[21] K. Ritos, I. W. Kokkinakis, D. Drikakis, Physical insight into the accuracy of finely-resolved iLES in turbulent boundary layers, Comput. Fluids 169 (2018) 309–316.

[22] P. D. Welch, The use of Fast Fourier Transform for the estimation of power spectra: A method based on time averaging over short, modified periodograms, IEEE Trans. Audio Electroacoust. AU-15 (1967) 70–73.

[23] D. A. Bies, A review of flight and wind tunnel measurements of boundary layer pressure fluctuations and induced structural response, Tech. Rep. CR-626, NASA (1966).

[24] J. E. Robertson, Prediction of in-flight fluctuating pressure environments including protuberance induced flow, Tech. Rep. CR-119947, NASA (1971).

[25] J. A. Cockburn, J. E. Robertson, Vibration response of spacecraft shrouds to in-flight fluctuating pressures, J. Sound Vib. 33 (4) (1974) 399–425.

[26] L. Duan, M. M. Choudhari, M. Wu, Numerical study of acoustic radiation due to supersonic turbulent boundary layer, J. Fluid Mech. 746 (2014) 165–192.

[27] L. Duan, M. M. Choudhari, C. Zhang, Pressure fluctuations induced by a hypersonic turbulent boundary layer, J. Fluid Mech. 804 (2016) 578–607.

[28] W. K. Blake, Mechanics of Flow-Induced Sound and Vibration, New York: Academic Press, 1986.

[29] M. K. Bull, Wall-pressure fluctuations beneath turbulent boundary layers: Some reflections on forty years of research, J. Sound Vib. 190 (3) (1996) 299–315.

[30] S. P. Gravante, A. M. Naguip, C. E. Wark, H. M. Nagib, Characterization of the pressure fluctuations under a fully developed turbulent boundary layer, AIAA Journal 36 (10) (1998) 1808–1816.

[31] T. M. Farabee, M. J. Casarella, Spectral features of wall pressure fluctuations beneath turbulent boundary layers, Phys. Fluids A 3 (10) (1991) 2410–2420.

[32] W. W. Willmarth, F. W. Roos, Resolution and structure of the wall pressure field beneath a turbulent boundary layer, J. Fluid Mech. 22 (1) (1965) 81–94.

[33] B. M. Efimtsov, Characteristics of the field of turbulent wall pressure fluctuations at large Reynolds numbers, Soviet Physics - Acoustics 28 (4) (1982) 289–292.

[34] B. M. Efimtsov, Similarity criteria for the spectra of wall pressure fluctuations in a turbulent boundary layer, Soviet Physics - Acoustics 30 (1) (1984) 33–35.

[35] B. M. Efimtsov, N. M. Kozlov, S. V. Kravchenko, A. O. Andersson, Wall pressure fluctuation spectra at small forward-facing steps, in: 5th AIAA/CEAS Aeroacoustics Conference and Exhibit, 1999.

[36] J. V. Blitterswyk, J. Rocha, Prediction and measurement of flow-induced wall-pressure fluctuations at low mach numbers, Canadian Acoustics 42 (4).

[37] F. Schultz-Grunow, New frictional resistance law for smooth plates, Tech. Rep. NACA-TM-986, NASA (1941).

[38] D. M. Chase, Modeling the wavevector-frequency spectrum of turbulent boundary layer wall pressure, J. Sound Vib. 70 (1980) 29–67.

[39] R. H. Kraichnan, Pressure fluctuations in turbulent flow over a flat plate, J. Acoust. Soc. Am. 28 (3) (1956) 378–390.

[40] Y. F. Hwang, W. K. Bonness, S. A. Hambric, Comparison of semi-empirical models for turbulent boundary layer wall pressure spectra, J. Sound Vib. 319 (2009) 199–217.

[41] A. V. Smol'yakov, V. M. Tkachenko, Model of a field of pseudosonic turbulent wall pressures and experimental data, Soviet Physics - Acoustics 37 (6) (1991) 627–631.

[42] S. J. Beresh, J. F. Henfling, R. W. Spillers, B. O. M. Pruett, Fluctuating wall pressures measured beneath a supersonic turbulent boundary layer, Phys. Fluids 23 (075110) (2011) 1–16.

[43] M. S. Howe, Acoustics of Fluid-Structure Interactions, Cambridge University Press, 1998.

[44] W. K. Blake, Turbulent boundary layer wall pressure fluctuations on smooth and rough walls, J. Fluid Mech. 44 (1970) 637–660.

[45] M. C. Goody, R. L. Simpson, Surface pressure fluctuations beneath two= and three-dimensional turbulent boundary layers, AIAA Journal 38 (10) (2000) 1822–1831.

[46] B. E. McGrath, R. L. Simpson, Some features of surface pressure fluctuations in turbulent boundary layers with zero and favorable pressure gradients, Tech. Rep. CR-4051, NASA (1987).

[47] P. Olivero-Bally, B. B. Forestier, E. Focquenoy, P. Olivero, Wall-pressure fluctuations in natural and manipulated turbulent boundary layers in air and water, in: FED/Flow noise modeling, measurement, and control, Vol. 168, ASME, 1993.

[48] G. Schewe, On the Structure and Resolution of Wall-Pressure Fluctuations Associated with Turbulent Boundary Layer Flow, J. Fluid Mech. 134 (1983) 311–328.

[49] Y. Rozenberg, G. Robert, S. Moreau, Wall-pressure spectral model including the adverse pressure gradient effects, AIAA Journal 50 (10) (2012) 2168–2179.